International Journal of Heat and Mass Transfer 52 (2009) 4358–4370

Contents lists available at ScienceDirect

International Journal of Heat and Mass Transfer

journal homepage: www.elsevier.com/locate/ijhmt

# Airside characteristics of heat, mass transfer and pressure drop for heat exchangers of tube-in hydrophilic coating wavy fin under dehumidifying conditions

Xiaokui Ma [a], Guoliang Ding [a,*], Yuanming Zhang [a], Kaijian Wang [b]

[a] Institute of Refrigeration and Cryogenics, Shanghai Jiaotong University, No. 800 Dongchuan Road, Shanghai 200240, China
[b] Fujitsu General Institute of Air-Conditioning Technology Limited, 1116 Suenaga, Takatsu-Ku, Kawasaki 213-8502, Japan

ARTICLE INFO

*Article history:*
Received 14 August 2007
Received in revised form 13 January 2009
Accepted 31 March 2009
Available online 15 May 2009

*Keywords:*
Dehumidifying conditions
Heat
Hydrophilic coating
Mass
Momentum
Wavy fin

ABSTRACT

The airside heat, mass and momentum transfer characteristics of seven wavy fin-and-tube heat exchangers with hydrophilic coating under dehumidifying conditions were experimented. The test inlet air dry bulb temperatures were 20, 27 and 35 °C, the inlet relative humidity were 50%, 60%, 70% and 80%, and the air velocity were 0.5, 1.0, 2.0, 3.0 and 4.0 m $s^{-1}$. The test results indicate that both the Colburn $j_m$ factor and the Colburn $j_h$ factor decrease with the increase of fin pitch, and this phenomenon becomes more and more pronounced as Reynolds number decreases. The friction factor is very sensitive to the change of fin pitch, and the friction factor shows a cross-over phenomenon as fin pitch changes. The Colburn $j_h$ factor decreases and the Colburn $j_m$ factor increases when the number of tube rows increases, while the friction performance is insensitive to the change of the number of tube rows. The effects of inlet relative humidity on the heat transfer and friction performance can be omitted, but the Colburn $j_m$ factor decreases with the increase of the inlet relative humidity. The predictive ability of the available state-of-the-art heat transfer and pressure drop correlations was evaluated with the experiment data of the present study. The new heat, mass and momentum transfer correlations were proposed to describe the present test results according to the multiple linear regression technique. The mean deviations of the proposed $j_h$, $j_m$ and $f$ correlations are 6.3%, 8.9% and 7.9%, respectively. Comparing to published data reduction method, the process line on psychrometric chart of fin-and-tube heat exchanger for partially wet conditions and more accurate overall heat transfer coefficient equation are put forward in this paper.
© 2009 Elsevier Ltd. All rights reserved.

## 1. Introduction

Fin-and-tube heat exchangers are essential components in air conditioning and refrigeration systems. Enhanced surface are often employed to effectively improve the overall performance of the fin-and-tube heat exchangers. Wavy fins are among the very popular enhanced fin patterns. The wavy surface can lengthen the path of the airflow and cause better airflow mixing, resulting in higher heat transfer performance.

When the surface temperature is below the dew point temperature of incoming air, simultaneous heat and mass transfer occurs on the fin surface, and condensate water is formed. The airflow across the heat exchanger may interact with the condensate water which makes the flow pattern become very complicated. As a result, significant change of the heat/mass transfer and friction characteristics is likely to occur under dehumidifying conditions. However, experimental data for dehumidifying conditions are comparatively few. Mirth and Ramadhyani [1,2] presented test results for five smooth wavy fin patterns. Their results showed that the Nusselt numbers were very sensitive to the change of inlet air dew point temperature, and the Nusselt number decreases with the increase of inlet air dew point temperature. Wang et al. [3], Lin et al. [4] and Pirompugd et al. [5] analyzed the effects of the number of tube rows, fin pitch and tube size, etc. on airside performance for herringbone wavy fin patterns in wet conditions, and developed their airside heat transfer and friction correlations.

The above-mentioned researches are focused on the wavy fin without hydrophilic coating. The condensate water may adhere as droplets on the fin surfaces without hydrophilic coating, and this phenomenon will cause bridging between the fins and increase airside pressure drop. Furthermore, the condensate water may corrode aluminum fins, and produce corrosion problems. A solution to solve this problem is to add hydrophilic coating on the aluminum fins. The hydrophilic coating can effectively improve the condensate water drainage and decrease airside pressure drop. Information on the effects of hydrophilic coating on the thermal/hydraulic performances of the fin-and-tube heat exchangers is also rare in open literatures. Mimaki [6] showed that the airside pressure drop of the coils under wet conditions was reduced up to 20–50% by using hydrophilic coated fins.

* Corresponding author. Tel.: +86 21 34206378; fax: +86 21 34206814.
*E-mail address:* glding@sjtu.edu.cn (G. Ding).

0017-9310/$ - see front matter © 2009 Elsevier Ltd. All rights reserved.
doi:10.1016/j.ijheatmasstransfer.2009.03.066

**Nomenclature**

| | |
|---|---|
| $a$ | coefficient defined by Eq. (A7) |
| $A_1$ | outside surface area of tubes ($m^2$) |
| $A_2$ | surface area of fin ($m^2$) |
| $A_{fr}$ | frontal area ($m^2$) |
| $A_{min}$ | minimum free-flow area ($m^2$) |
| $A_0$ | total airside surface area ($m^2$) |
| $b$ | coefficient defined by Eq. (A7) |
| $C_p$ | specific heat ($J\,kg^{-1}\,K^{-1}$) |
| $D_c$ | fin collar outside diameter (m) |
| $f$ | friction factor |
| $F_p$ | fin pitch (m) |
| $F_s$ | fin spacing (m) |
| $G_c$ | mass flux of the air based on the minimum flow area ($kg\,m^{-2}\,s^{-1}$) |
| $h_m$ | mass transfer coefficient ($kg\,m^{-2}\,s^{-1}$) |
| $h_s$ | sensible heat transfer coefficient ($W\,m^{-2}\,K^{-1}$) |
| $i$ | enthalpy ($kJ\,kg^{-1}$) |
| $i_{fg}$ | saturated water vapor enthalpy ($kJ\,kg^{-1}$) |
| $I_0$ | modified Bessel function solution of the first kind, order 0 |
| $I_1$ | modified Bessel function solution of the first kind, order 1 |
| $j_h$ | Colburn heat transfer factor |
| $j_m$ | Colburn mass transfer factor |
| $k$ | thermal conductivity ($W\,m^{-1}\,K^{-1}$) |
| $K_0$ | modified Bessel function solution of the second kind, order 0 |
| $K_1$ | modified Bessel function solution of the second kind, order 1 |
| Le | Lewis number |
| $m$ | mass flow rate ($kg\,s^{-1}$) |
| $m^*$ | coefficient defined by Eq. (A15) |
| $M$ | condensate rate ($kg\,s^{-1}$) |
| $M_{fb}$ | coefficient defined by Eq. (A3) |
| $M^*$ | coefficient defined by Eq. (A2) |
| N | number of longitudinal tube rows |
| $P_l$ | longitudinal tube pitch (m) |
| $Pr$ | Prandtl number |
| $P_t$ | transverse tube pitch (m) |
| $\Delta P$ | pressure drop of airside (Pa) |
| $Q$ | average heat transfer rate (W) |
| $Q_s$ | sensible heat transfer rate (W) |
| $Q_l$ | latent heat transfer rate (W) |
| $r$ | fin radius (m) |
| $Re_{Dc}$ | Reynolds number based on tube collar diameter |
| $RH$ | relative humidity |
| $Sc$ | Schmidt number |
| $T$ | temperature (K) |
| $T_a^*$ | coefficient defined by Eq. (A4) |
| $V$ | velocity ($m\,s^{-1}$) |
| $W$ | humidity ratio of moist air ($kg\,kg^{-1}$) |

*Greek symbols*

| | |
|---|---|
| $\beta$ | coefficient defined by Eq. (A5) |
| $\delta$ | fin thickness (m) |
| $\eta_{f,h,wet}$ | wet fin efficiency for heat transfer |
| $\eta_{f,m}$ | fin efficiency for mass transfer |
| $\eta_o$ | overall surface effectiveness |
| $\xi$ | boundary line between dry region and wet region |

*Subscripts*

| | |
|---|---|
| a | air |
| d | dew point |
| dry | dry bulb temperature |
| f | fin |
| fb | fin base |
| ft | fin tip |
| i | inner |
| in | inlet |
| o | outer |
| out | outlet |
| s | saturated |
| w | water |

Hong [7] presented a fundamental aspect to the hydrophilic coating surfaces. Among the methods of coating the aluminum fins, as documented by Hong and Webb [8], chemical methods are adopted as the main-stream methods. Hong and Webb [9] did researches on enhanced fin-and-tube heat exchangers with and without hydrophilic coating. The results showed that hydrophilic coating would reduce the pressure drop. For wet coils, the hydrophilic coating applied on the louver and wavy fin reduces the wet pressure drop to 45% and 15% at 2.5 $m\,s^{-1}$ frontal air velocity, respectively. The airside performance comparison of plain, louver, and slit fin-and-tube heat exchangers with and without hydrophilic coating were examined by Wang et al. [10,11]. The results showed that the heat transfer performance for the hydrophilic coating surface is lower than that for the corresponding uncoated surface tested at the same wet conditions, and the pressure drops for the hydrophilic coated surface are also lower than the corresponding uncoated surfaces.

Until now, no data on the wavy fin-and-tube heat exchangers with hydrophilic coating under wet conditions have been published in open literatures. As a consequence, the main purpose of this study is to present airside heat, mass and momentum transfer performance of wavy fin-and-tube heat exchanger with hydrophilic coating under dehumidifying conditions, which may give helps in design of wavy fin-and-tube heat exchangers.

## 2. Experimental apparatus

The experimental apparatus is schematically illustrated in Fig. 1, which includes an air flow loop, a water flow loop, a data acquisition system and the test heat exchangers.

The air flow loop is a close type wind tunnel to conduct the air flow through the heat exchanger. The wind tunnel is made of galvanized steel sheet and the test section has a 210 mm × 210 mm cross-section. A variable speed centrifugal fan (0.75 kW) is used to circulate the air passing through the nozzle chamber, the air conditioner box, the mixing device, the straightener, and the test heat exchanger orderly. The air flow rate measurement is detected by multiple nozzles based on the ASHRAE 41.2 standard [12]. A differential pressure transducer with ±5.0 Pa precision is used to measure the pressure difference across the nozzles. A pressure transducer with ±1.0 kPa precision and a dry bulb and wet bulb temperature transducer with ±0.3 °C precision are used to measure the inlet air conditions of nozzles. The air conditioner box is used to control the temperature and humidity of inlet air, which are allowed ±0.2 °C and ±3% fluctuation range. The test section is insulated with a 15 mm thick standard sheet. A differential pressure transducer with ±0.2 Pa precision is used to measure the pressure difference across the heat exchangers. The dry bulb temperature and relative humidity of the inlet and outlet air are measured by

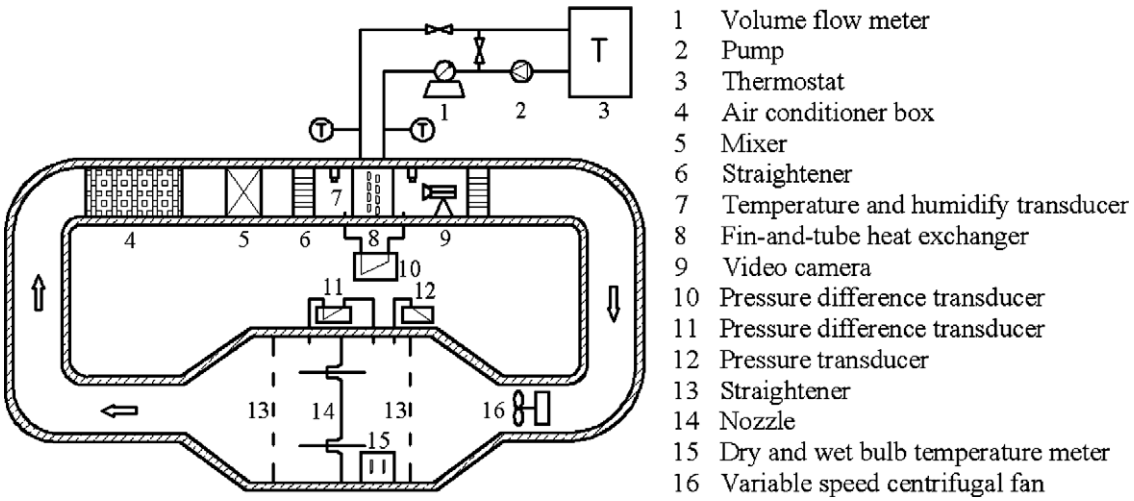


**Fig. 1.** Schematic of experimental setup.

two temperature and humidity transducers with ±0.1 °C and ±1.4% precision. Six K-type thermocouples with ±0.1 °C precision welded on the tube surface are used to measure the fin base temperature.

The water flow loop consists of a thermostat, a centrifugal pump and a magnetic flow meter with ±0.15 L/min precision. The purpose of this loop is to provide the cool capacity of the test heat exchangers. After the water reaches the required temperature, it is pumped out of the thermostat, delivered to the heat exchanger and then returned to the thermostat. The water temperature differences between inlet and outlet of heat exchangers are measured by two K-type thermocouples with a calibrated accuracy of ±0.1 °C. All signals are registered by a data acquisition system and finally averaged over the elapsed time.

Seven fin-and-tube heat exchangers for testing are made of aluminum fin and copper tube. Detailed dimensions of the heat exchangers and the fins are shown in Fig. 2. Their detailed configurations are tabulated in Table 1. Fin surface coatings include anti-corrosive layer and hydrophilic layer. The coating material is organic resin, the thickness of anti-corrosive layer and hydrophilic layer is 1.1 μm and 0.8 μm, and the static contact angle on the

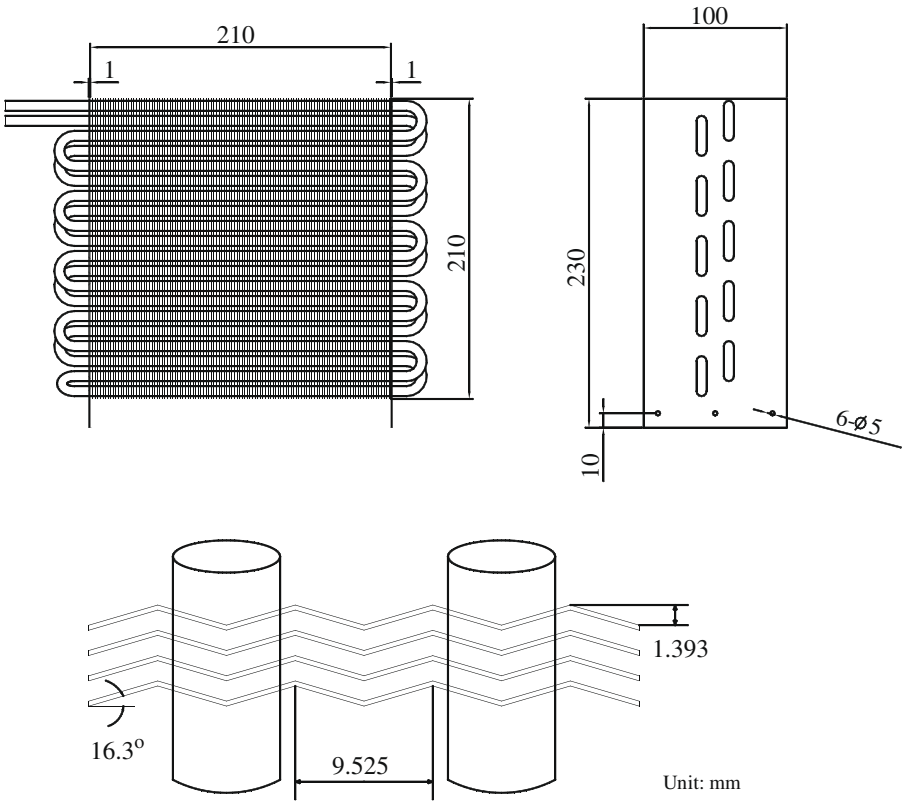


**Fig. 2.** Structure dimensions of the tested fin-and-tube heat exchangers.

**Table 1**
Geometric dimension of the test fin-and-tube heat exchangers.

| No. | $F_p$ (mm) | $\delta$ (mm) | $D_c$ (mm) | $P_t$ (mm) | $P_l$ (mm) | $P_d$ (mm) | $X_f$ (mm) | $N$ |
|---|---|---|---|---|---|---|---|---|
| 1 | 1.2 | 0.105 | 7.51 | 21.0 | 19.05 | 1.352 | 4.625 | 2 |
| 2 | 1.5 | 0.105 | 7.51 | 21.0 | 19.05 | 1.352 | 4.625 | 2 |
| 3 | 1.7 | 0.105 | 7.51 | 21.0 | 19.05 | 1.352 | 4.625 | 2 |
| 4 | 1.4 | 0.105 | 10.31 | 25.4 | 19.05 | 1.352 | 4.625 | 2 |
| 5 | 1.8 | 0.105 | 10.31 | 25.4 | 19.05 | 1.352 | 4.625 | 2 |
| 6 | 1.5 | 0.105 | 7.51 | 21.0 | 19.05 | 1.352 | 4.625 | 3 |
| 7 | 1.4 | 0.105 | 10.31 | 25.4 | 19.05 | 1.352 | 4.625 | 3 |

*Note:* $D_c$ is the tube outside diameter (including collar thickness) after expansion.

coated fin surface is 10°–20° initially. Coating process chart of fin is shown in Fig. 3.

Condensation phenomena on the fin surface are recorded by a video camera put at the outlet of air. Total 23 test conditions are listed in Table 2. Experiment uncertainties are reported according to the analysis method proposed by Moffat [13], and the maximum error of the Colburn $j_h$ factor and Fanning $f$ factor are ±10.2% and ±9.4%, respectively. The detailed analysis results are tabulated in Table 3.

## 3. Data reduction

### 3.1. Heat transfer data

The reduction process is based on the Threlkeld [14] method. The Threlkeld method is an enthalpy-based reduction method. Some important reduction procedures of the original Threlkeld method are described as follows:

The total heat transfer rate used in the calculation is the mathematical average of $Q_a$ and $Q_w$, namely,

$$Q_a = m_a(i_{a,in} - i_{a,out}) \tag{1}$$

$$Q_w = m_w C_{p,w}(T_{w,out-T_{w,in}}) \tag{2}$$

$$Q = (Q_a + Q_w)/2 \tag{3}$$

In the experiments, only those data that satisfy the ASHRAE 33-78 [15] requirements (namely, the energy balance conditions, $|Q_w - Q|/Q \leqslant 0.05$) are considered in the final analysis.

The overall heat transfer coefficient ($U_{o,w}$) based on the enthalpy potential is given as follows:

$$Q = U_{o,w}A_0\Delta i_m F \tag{4}$$

where $F$ is the correction factor accounting for a single-pass, cross-flow heat exchanger and $\Delta i_m$ is the mean enthalpy difference for counter flow coil.

$$\Delta i_m = i_{a,m} - i_{r,m} \tag{5}$$

According to Bump [16] and Myers [17], for the counter flow configuration, the mean enthalpy difference is

$$i_{a,m} = i_{a,in} + \frac{i_{a,in} - i_{a,out}}{\ln\left(\frac{i_{a,in}-i_{r,out}}{i_{a,out}-i_{r,in}}\right)} - \frac{(i_{a,in} - i_{a,out})(i_{a,in} - i_{r,out})}{(i_{a,in} - i_{r,out}) - (i_{a,out} - i_{r,in})} \tag{6}$$

$$i_{r,m} = i_{r,out} + \frac{i_{r,out} - i_{r,in}}{\ln\left(\frac{i_{a,in}-i_{r,out}}{i_{a,out}-i_{r,in}}\right)} - \frac{(i_{r,out} - i_{r,in})(i_{a,in} - i_{r,out})}{(i_{a,in} - i_{r,out}) - (i_{a,out} - i_{r,in})} \tag{7}$$

According to the definition of wet fin efficiency by Threlkeld [14] based on the enthalpy difference, Myers [17] reduced the overall heat transfer coefficient related to the individual heat transfer resistance as follows:

$$\frac{1}{U_{o,w}} = \frac{b'_r A_0}{h_i A_{p,i}} + \frac{b'_p A_0 \ln\left(\frac{D_c}{D_i}\right)}{2\pi k_p L_p} + \frac{1}{h_{o,w}\left(\frac{A_{p,o}}{b'_{w,p}A_o} + \frac{\eta_{f,wet}A_f}{b'_{w,m}A_o}\right)} \tag{8}$$

where

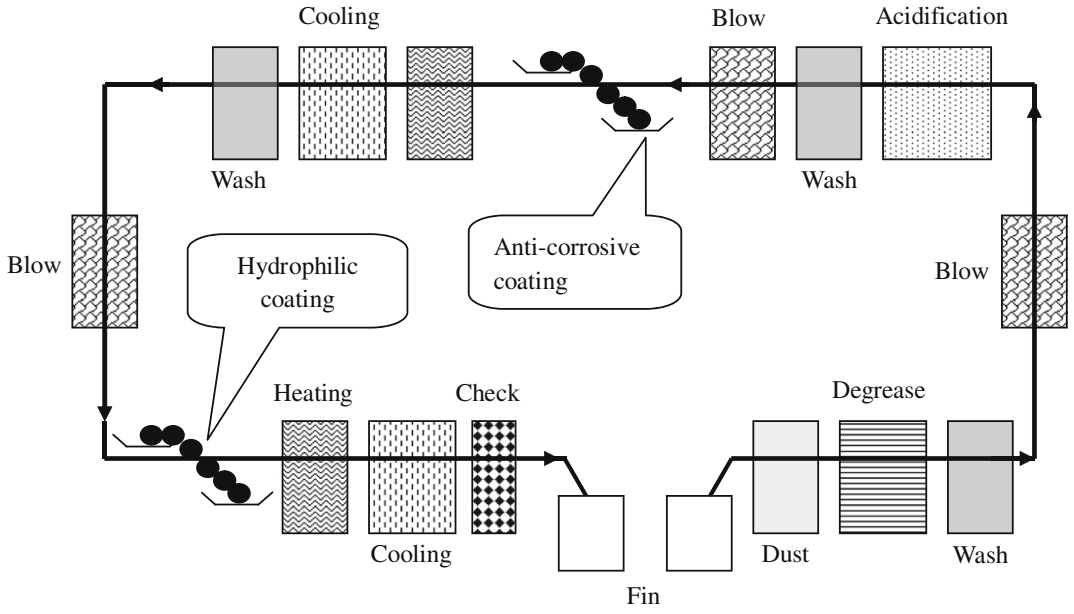


**Fig. 3.** Coating process of fin surface.

**Table 2**
The test conditions of experiment.

| No. | $T_{a,in}$/°C | $RH_{in}$/% | $V$/(m s$^{-1}$) | $T_{w,in}$/°C |
|---|---|---|---|---|
| 1 | 20 | 50 | 0.5 | 6 |
| 2 | 20 | 50 | 1.0 | 6 |
| 3 | 20 | 50 | 2.0 | 6 |
| 4 | 27 | 50 | 1.0 | 6 |
| 5 | 27 | 60 | 1.0 | 6 |
| 6 | 27 | 70 | 1.0 | 6 |
| 7 | 27 | 80 | 1.0 | 6 |
| 8 | 27 | 50 | 0.5 | 12 |
| 9 | 27 | 50 | 1.0 | 12 |
| 10 | 27 | 50 | 2.0 | 12 |
| 11 | 27 | 50 | 3.0 | 12 |
| 12 | 27 | 50 | 4.0 | 12 |
| 13 | 35 | 50 | 0.5 | 12 |
| 14 | 35 | 50 | 1.0 | 12 |
| 15 | 35 | 50 | 2.0 | 12 |
| 16 | 35 | 50 | 3.0 | 12 |
| 17 | 35 | 50 | 4.0 | 12 |
| 18 | 27 | 60 | 1.0 | 12 |
| 19 | 27 | 70 | 1.0 | 12 |
| 20 | 27 | 80 | 1.0 | 12 |
| 21 | 27 | 60 | 1.0 | 18 |
| 22 | 27 | 70 | 1.0 | 18 |
| 23 | 27 | 80 | 1.0 | 18 |

**Table 3**
Summary of estimated uncertainties.

| Parameter | Uncertainty | | Parameter | Uncertainty | |
|---|---|---|---|---|---|
| | Min (%) | Max (%) | | Min (%) | Max (%) |
| $m_a$ | ±0.9 | ±1.8 | $h_s$ | ±6.0 | ±8.4 |
| $m_w$ | ±1.5 | ±2.5 | $h_m$ | ±5.1 | ±7.8 |
| $Q_a$ | ±1.8 | ±3.9 | $j_h$ | ±6.9 | ±10.2 |
| $Q_w$ | ±2.5 | ±5.0 | $j_m$ | ±6.3 | ±11.3 |
| $\Delta P$ | ±0.1 | ±4.0 | $f$ | ±3.7 | ±9.4 |

$$h_{o,w} = \frac{1}{\frac{C_{p,a}}{b'_{w,m}h_{c,o}}} + \frac{y_w}{k_w} \tag{9}$$

$y_w$ in Eq. (9) is the thickness of the water film, and was proposed as 0.005 in. by Myers [17]. In practice, $(y_w/k_w)$ accounts for only 0.5–5% compared to $(C_{p,a}/b'_{w,m}h_{c,o})$, and has often been neglected by previous investigators. As a result, this term is not included in the final analysis.

In Eq. (8) there are four quantities ($b'_{w,m}$, $b'_{w,p}$, $b'_p$, and $b'_r$) involving enthalpy–temperature ratios that must be evaluated. The quantities of $b'_p$ and $b'_r$ can be calculated as

$$b'_r = \frac{i_{s,p,i,m} - i_{r,m}}{T_{p,i,m} - T_{r,m}} \tag{10}$$

$$b'_p = \frac{i_{s,p,o,m} - i_{s,p,i,m}}{T_{p,o,m} - T_{p,i,m}} \tag{11}$$

The $b'_{w,p}$ and $b'_{w,m}$ are defined as the slope of saturated enthalpy curve evaluated at the outer mean water film temperature at the base surface and the fin surface by Threlkeld [14]. However, according to the Threlkeld's analysis method [14], $b'_{w,p}$ and $b'_{w,m}$ should be defined as the slope of saturated enthalpy curve evaluated at the outside surface temperature of tube and at the fin surface mean temperature, and this definition is more appropriate. Evaluation of $b'_{w,m}$ requires a trial and error procedure, for the trial and error procedure, $i_{s,w,m}$ must be calculated using the following equation:

$$i_{s,w,m} = i_{a,m} - \frac{C_{p,a}h_{o,w}\eta_{f,wet}}{b'_{w,p}h_{c,o}}\left(1 - U_{o,w}A_o\left[\frac{b'_r}{h_iA_{p,i}} + \frac{b'_p \ln\left(\frac{D_c}{D_i}\right)}{2\pi k_p L_p}\right]\right)(i_{a,m} - i_{r,m}) \tag{12}$$

Wang et al. [18] also used Eq. (8) in their research on fin-and-tube heat exchanger under dehumidifying conditions. Threlkeld [14] made a approximation $b'_{f,b} = b'_{w,m}$ during the definition of the wet fin efficiency, and the equation proposed by Threlkeld is as follows:

$$\eta_{f,wet} = \frac{i_a - i_{f,m}}{i_a - i_{f,b}} \tag{13}$$

When the approximation is removed, the more accurate definition of the wet fin efficiency should be as follows:

$$\eta_{f,wet} = \left(\frac{i_a - i_{f,m}}{i_a - i_{f,b}}\right)\frac{b'_{f,b}}{b'_{w,m}} \tag{14}$$

where the value of $b'_{f,b}$ is the slope of saturated enthalpy curve evaluated at the fin base temperature. Because the outside surface temperature of tube can be equal to the fin base temperature approximatively, we make the approximation $b'_{f,b} = b'_{w,p}$, and more accurate overall heat transfer coefficient can be gotten as follows:

$$\frac{1}{U_{o,w}} = \frac{b'_r A_o}{h_i A_{p,i}} + \frac{b'_p A_o \ln\left(\frac{D_c}{D_i}\right)}{2\pi k_p L_p} + \frac{b'_{w,p}A_o}{h_{o,w}(A_{p,o} + \eta_{f,wet}A_f)} \tag{15}$$

The tube side heat transfer coefficient, $h_i$ is evaluated from the Gnielinski correlation [19],

$$h_i = \frac{(f_i/2)(Re_{Di} - 1000)Pr}{1.07 + 12.7\sqrt{f_i/2}\left(Pr^{2/3} - 1\right)} \cdot \frac{k_i}{D_i} \tag{16}$$

and the friction factor $f_i$ is

$$f_i = \frac{1}{(1.58\ln Re_{Di} - 3.28)^2} \tag{17}$$

where

$$Re_{Di} = (\rho_w V_w D_i)/\mu_w \tag{18}$$

For the wet fin efficiency, Wang et al. [18] derived the corresponding formula by the equivalent circular area method

$$\eta_{f,wet} = \frac{2r_i}{M_T(r_o^2 - r_i^2)} \times \left[\frac{K_1(M_T r_i)I_1(M_T r_o) - I_1(M_T r_i)K_1(M_T r_o)}{K_0(M_T r_i)I_1(M_T r_o) + K_1(M_T r_o)I_0(M_T r_i)}\right] \tag{19}$$

where

$$M_T = \sqrt{\frac{2h_{o,w}}{k_f\delta_f}} \tag{20}$$

But Eq. (19) can only be used in fully wet conditions. For partially wet conditions, the use of Eq. (19) will bring big error. In this regard, the authors analyzed wet fin efficiency $\eta_{f,wet}$, and listed the detailed reduction process and comparison with other fin efficiency correlations in the literature. Ma [20]. The calculation correlations of wet fin efficiency $\eta_{f,wet}$ are listed in Appendix A.

The heat transfer performance is in terms of the Colburn $j_h$ factor, i.e.,

$$j_h = \frac{h_{c,o}}{G_c C_{p,a}} Pr^{2/3} \tag{21}$$

where

$$G_c = \frac{m_a}{A_{min}} \tag{22}$$

### 3.2. Mass transfer data

For the cooling and dehumidifying of moist air by a cold surface, the heat and mass transfer can be described by the process line equation from Threlkeld [14]:

$$\frac{di_a}{dW_a} = R\frac{(i_a - i_{s,w})}{(W_a - W_{s,w})} + (i_{fg} - 2501R) \tag{23}$$

where $R$ represent the ratio of sensible heat transfer characteristics to the mass transfer performance,

$$R = \frac{h_{c,o}}{h_{d,o}C_{p,a}} \tag{24}$$

However, for the fin-and-tube heat exchanger, Eq. (23) does not correctly describe the dehumidification process on the psychometric chart because the saturated air enthalpy ($i_{s,w}$) at the mean temperature at the fin surface is different from that at the fin base. In this regard, Pirompugd [5] put forward a modification process line on the psychometric chart corresponding to the fin-and-tube heat exchanger.

$$\frac{(i_{a,in} - i_{a,out})}{(W_{a,in} - W_{a,out})} = R \cdot \frac{(i_{a,m} - i_{s,p,o,m}) + (\varepsilon - 1)(i_{a,m} - i_{s,w,m})}{(W_{a,m} - W_{s,p,o,m}) + (\varepsilon - 1)(W_{a,m} - W_{s,w,m})} \tag{25}$$

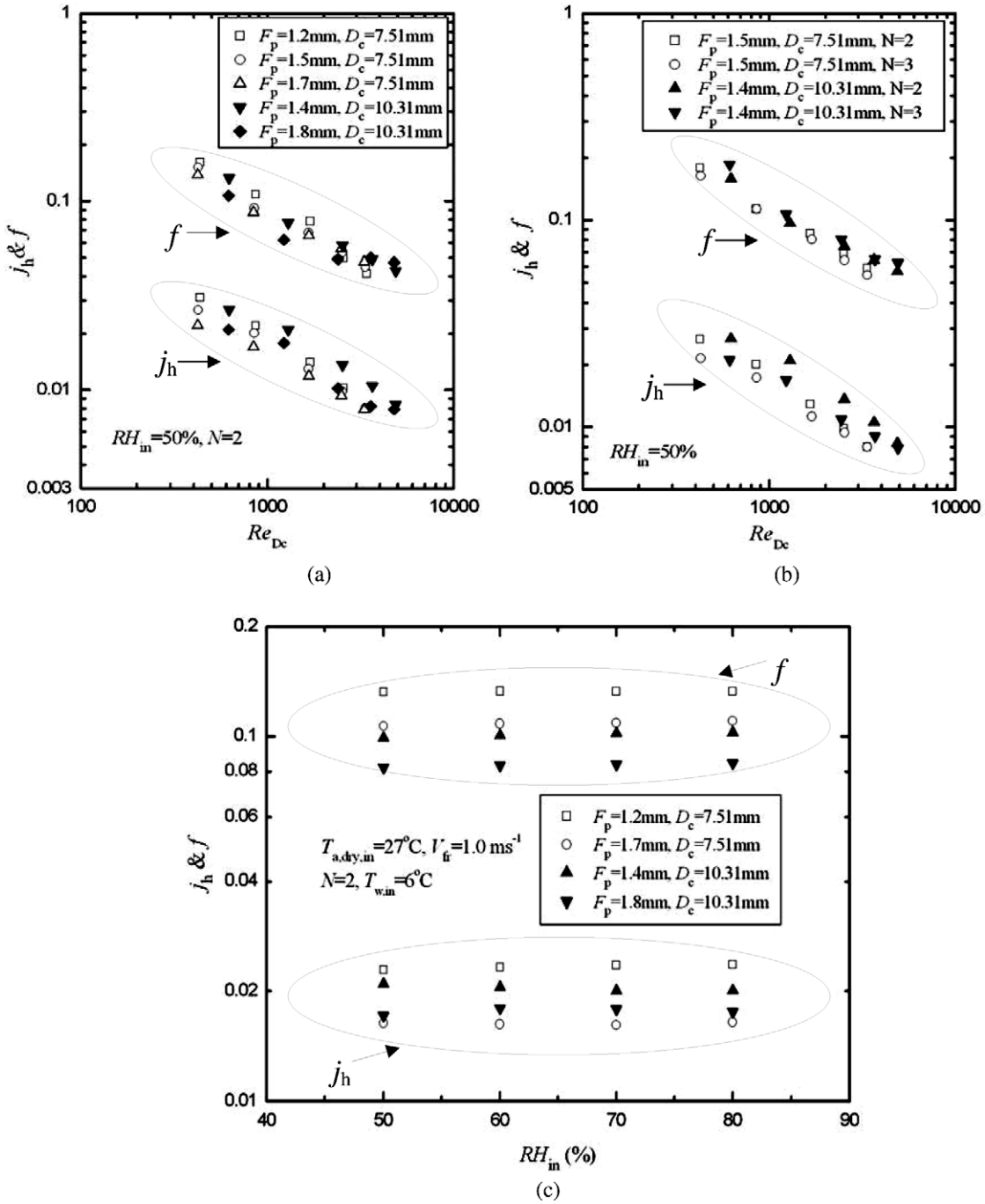


**Fig. 4.** Effect of the parameters on the airside heat and momentum transfer performance. (a) Fin pitch, (b) number of rows and (c) inlet relative humidity.

where

$$\varepsilon = \frac{A_0}{A_{p,o}} \tag{26}$$

But Eq. (25) is only suitable for fully wet conditions. In this paper, the process line on psychrometric chart of fin-and-tube heat exchanger for partially wet conditions is put forward. The derivation is as follows:

From the energy balance of the dehumidification one can arrive at the following expression

$$m_a(i_{a,in} - i_{a,out}) = \frac{h_{o,w}}{b'_{w,p}}(A_{p,o} + \eta_{f,wet}A_f)(i_{a,m} - i_{s,p,o,m}) \tag{27}$$

Conservation of water condensate gives

$$m_a(W_{a,in} - W_{a,out}) = h_{d,o}[A_{p,o}(W_{a,m} - W_{s,p,o,m}) + A_{f,wet}(W_{a,m} - W_{s,w,m})] \tag{28}$$

Dividing Eq. (27) by Eq. (28) yields

$$\frac{(i_{a,in} - i_{a,out})}{(W_{a,in} - W_{a,out})} = R \cdot \frac{b'_{w,m}}{b'_{w,p}} \cdot \frac{(A_{p,o} + \eta_{f,wet}A_f)(i_{a,m} - i_{s,p,o,m})}{A_{p,o}(W_{a,m} - W_{s,p,o,m}) + A_{f,wet}(W_{a,m} - W_{s,w,m})} \tag{29}$$

The mass transfer performance is in terms of the Colburn $j_m$ factor, i.e.,

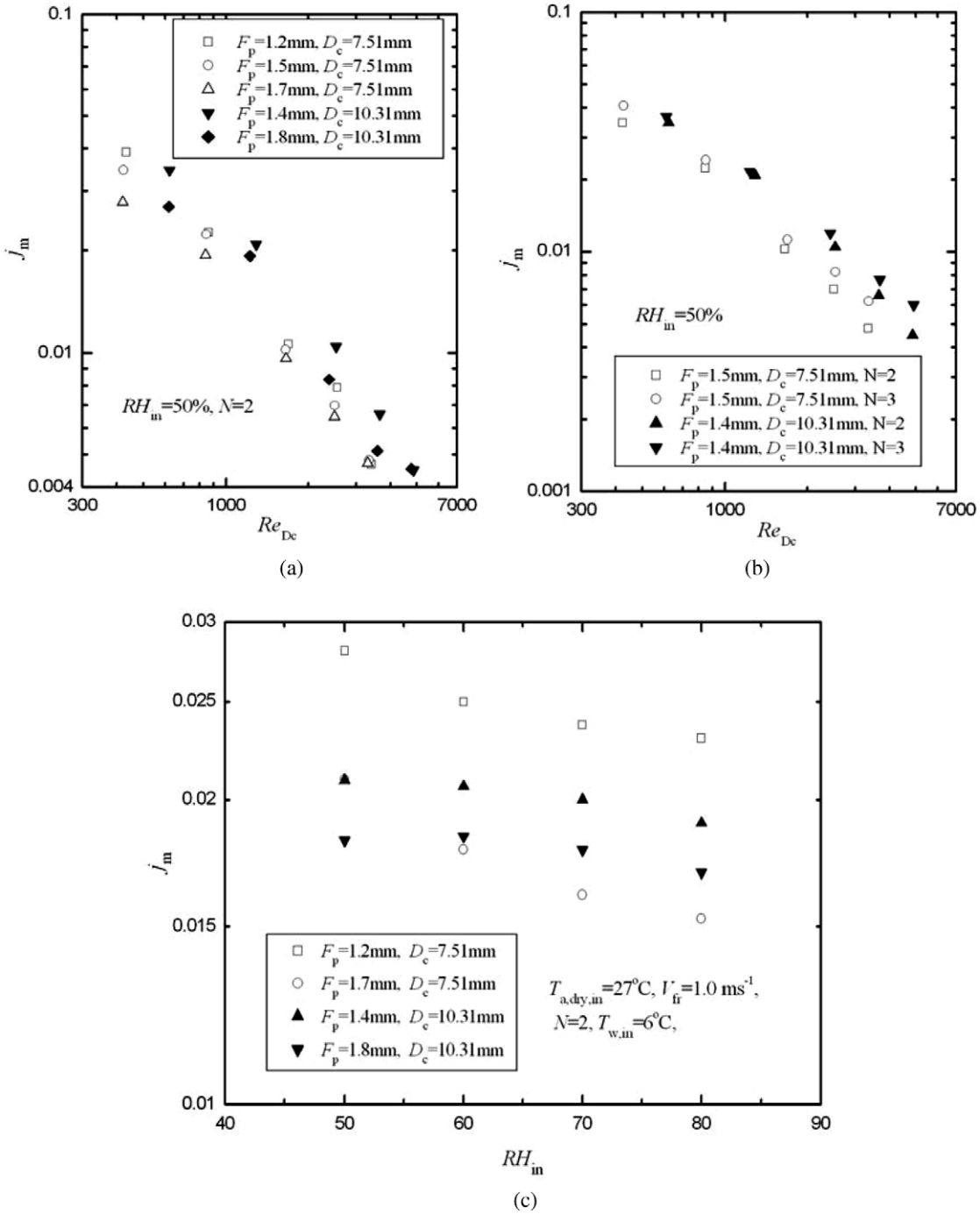


**Fig. 5.** Effect of the parameters on the airside mass transfer performance. (a) fin pitch (b) number of rows (c) inlet relative humidity.

$$j_m = \frac{h_{d,o}}{G_c} Sc^{2/3} \tag{30}$$

An algorithm for solving the Colburn $j_h$ factor and Colburn $j_m$ factor is given as follows:

(1) Based on the measurement data, calculate the total heat transfer rate $Q$ using Eq. (3).
(2) Calculate the tube side heat transfer coefficient of $h_i$ using Eq. (16).
(3) Calculate $i_{a,m}$ by Eq. (6) and $i_{r,m}$ by Eq. (7).
(4) Calculate $T_{p,i,m}$ and $T_{p,o,m}$.
(5) Assume a value of $R$.
(6) Assume a value of $h_{c,o}$.
(7) Calculate the wet fin efficiency $\eta_{f,wet}$.
(8) Calculate the $b'_p$ and $b'_r$.
(9) Calculate the overall heat transfer coefficient $U_{o,w}$.
(10) Assume a value of $T_{w,m}$.
(11) Calculate $i_{s,w,m}$ by Eq. (12).
(12) Calculate $T_{w,m}$ from $i_{s,w,m}$.
(13) If $T_{w,m}$ derived in step (12) is not equal that is assumed in step (10), the calculation steps (10)–(12) will be repeated with $T_{w,m}$ derived in step (12) until $T_{w,m}$ is constant.
(14) Calculate $h_{c,o}$ from Eq. (15).
(15) If $h_{c,o}$ derived in step (14) is not equal to that assumed in step (6), the calculation steps (6)–(14) will be repeated with $h_{c,o}$ derived in step (14) until $h_{c,o}$ is constant.
(16) Obtain $W_{s,p,o,m}$ and $W_{s,w,m}$ from $i_{s,p,o,m}$ and $i_{s,w,m}$.
(17) Calculate $R$ using Eq. (25) under fully wet conditions, and calculate $R$ using Eq. (29) under partially wet conditions.
(18) If $R$ derived in step (17) is not equal to that assumed in step (5), the calculation steps (5)–(17) will be repeated with $R$ derived in step (17) until $h_{c,o}$ is constant.
(19) Calculate $h_{d,o}$ by Eq. (24).
(20) Calculate the Colburn $j_h$ factor by Eq. (21) and Colburn $j_m$ factor by Eq. (30).

### 3.3. Momentum transfer data

The reduction of the Fanning $f$ factor of the heat exchanger is evaluated from the pressure drop equation proposed by Kays and London [21],

$$f = \frac{A_{min}}{A_0}\frac{\rho_m}{\rho_i}\left[\frac{2\Delta P \rho_i}{G_c^2} - (1+\sigma^2)\left(\frac{\rho_i}{\rho_o} - 1\right)\right] \tag{31}$$

where

$$\sigma = \frac{A_{min}}{A_{fr}} \tag{32}$$

## 4. Results and discussion

### 4.1. Analysis on heat and momentum transfer characteristics

Fig. 4(a) shows the effect of the fin pitch on the airside heat transfer and friction characteristics of wavy fin with hydrophilic coating. The ordinates are Colburn $j_h$ factors and Fanning $f$ factor, and the abscissa is the Reynolds number based on collar diameter. The inlet air dry bulb temperature is 27 °C, the inlet air relative humidity is 50%, the inlet water temperature is 12 °C, and the number of tube rows is 2. As shown in Fig. 4(a), the Colburn $j_h$ factors decrease with the increase of the fin pitch. This phenomenon is especially pronounced in low Reynolds number region. The trend is different with research results of plain, wavy and louver fin-and-tube heat exchanger having a 4-row configuration by Rich [22] and Wang et al. [18,23–26], whatever dry conditions or dehumidifying conditions. But for fin-and-tube heat exchanger having 1-row and 2-row configuration, the research results by Wang et al. [3,27] is similar to that of this paper, so the effect of the fin pitch on the airside heat transfer performance is relative to the number of tube rows. This phenomenon can be further explained by the 3D numerical investigation results obtained by Torikoshi et al. on a 1-row plain fin-and-tube heat exchanger [28]. The results show that the vortex that forms behind the tube can be suppressed and entire flow region can be kept steady and laminar when the fin pitch is small enough. Further increase of the fin pitch would result in a noticeable increase of cross-stream width of the vortex region behind the tube. The detailed explanations for this phenomenon can be found in the research by Wang et al. [27]. Fig. 4(a) also shows that the friction factors show a cross-over phenomenon as fin pitch changes, which is similar with the results under dry conditions [24].

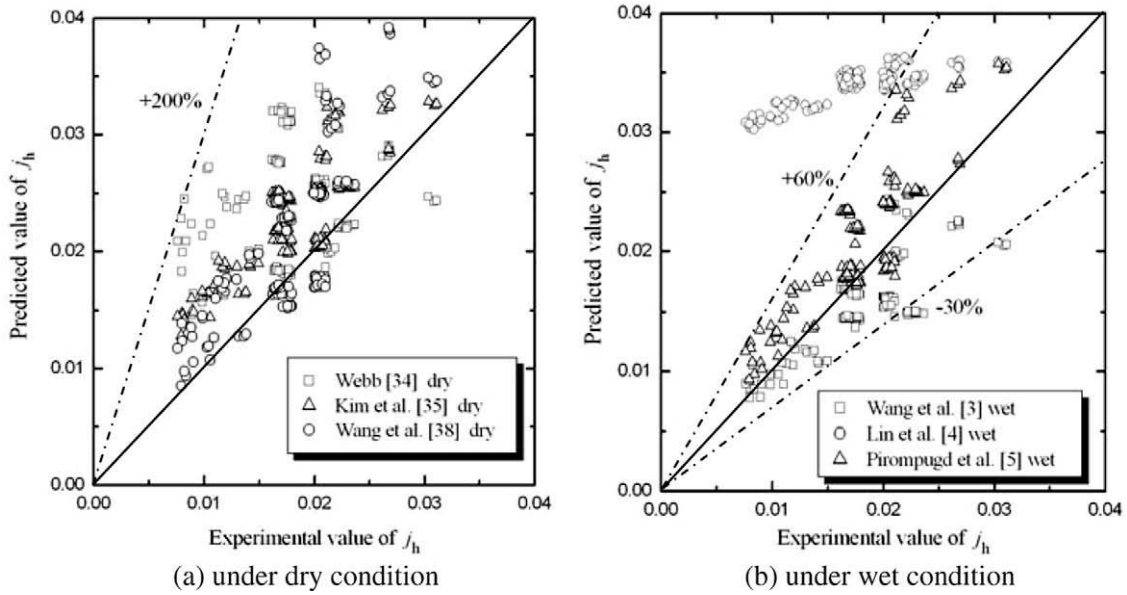


**Fig. 6.** Validation of existing heat transfer correlations with experiment data.

Fig. 4(b) depicts the effect of the number of tube rows on the airside performance of wavy fin-and-tube heat exchangers with hydrophilic coating. The ordinates are Colburn $j_h$ factors and Fanning $f$ factor, and the abscissa is the Reynolds number based on collar diameter. The Colburn $j$ factors decrease with the increase of the number of tube rows. This phenomenon is especially pronounced in low Reynolds number region. This trend is similar with the test results of plain fin-and-tube heat exchanger by Rich [29] and Wang et al. [23,27] under dry conditions and it is also similar with the results of plain fin and wavy fin by Wang et al. [3,18] under dehumidifying conditions. The possible explanations of this phenomenon are summarized as follows. The downstream turbulence is deteriorated by the vortices formed behind the tube row, and the downstream turbulence tends to diminish with the increase of the number of tube rows. When the Reynolds number decreases, the vortices behind the tube become more pronounced [23]. Fig. 4(b) also indicates that the friction factors are insensitive to the number of tube row for wavy fin with hydrophilic coating under dehumidifying condition. Because the condensate water can be drained by the hydrophilic coating in time, this phenomenon is very similar with the test results of fin-and-tube heat exchanger under dry conditions [23,24,29]. Wang et al. [3] made the airside performance experimental research of wavy fin-and-tube heat exchanger without hydrophilic coating under dehumidifying condition, and they found that the effect of the number of tube rows on the airside friction characteristic is very sensible. Their result is different from that of this paper, and this difference may be caused by the different dehumidification conditions on the fin surface between the coated fin and uncoated fin. For coated fin, water film will be formed on the fin surface; for uncoated fin, water droplets will be formed on the fin surface. When the fin pitch is close to each other, the droplets adhering to the fin surface may cause the airflow twisting. As humid air flows across the wet coils, the corresponding specific humidity decreases along the direction of the airflow, the local dew point temperatures decrease and the driving potential of mass transfer also decreases. The condensate water rate and twisted airflow may decrease as the number of tube rows increase. As a result, for the uncoated fin, the friction factors decrease with the increase of the number of tube rows; but for the coated fin, this phenomenon does not exist.

Fig. 4(c) shows the effect of the inlet relative humidity on the airside performance of wavy fin-and-tube heat exchanger with hydrophilic coating. The air dry bulb temperature $T_{a,dry} = 27\ ^{o}C$, the inlet air flow velocity $V_{a,in} = 1.0\ ms^{-1}$, and the corresponding number of tube rows is 2. As shown in Fig. 4(c), the Colburn $j$ factors and the friction factors are relatively insensitive to the change of inlet relative humidity. This is similar with the experimental results of plain fin, slit fin and louver fin by Wang et al. [18,30,31] and is different from the test result by Mirth and Ramadhyani [1,2] and Fu et al. [32]. Wang et al. [18] pointed out that the reason was that they chose different wet fin efficiency calculation equations.

### 4.2. Analysis on mass transfer characteristic

The effect of the fin pitch, the number of tube rows and the inlet relative humidity on the airside mass transfer characteristic are shown in Figs. 5(a)–(c), respectively. The ordinates are Colburn $j_m$ factor, and the abscissa is the Reynolds number based on collar diameter. Fig. 5(a) shows that the airside mass transfer characteristic of smaller fin pitch is better than that of larger fin pitch. The trend is similar with the results of wavy fin without hydrophilic coating by Pirompugd et al. [5]. Fig. 5(b) indicates that the Colburn $j_m$ factor increases with the increase of the number of tube row. This phenomenon can be explained by the flow visualization experiments conducted by Yoshii et al. [33] who tested a scale-up model under wet conditions. When humid air flows across the wet coils, the corresponding specific humidity decreases along the direction of the airflow. Hence, the local dew point temperatures also decrease and the driving potential of mass transfer is decreased. Thus, the water condensate rate may be decreased as the number of tube row increases. As a result, the water condensate decreases and the mass transfer performance become well with an increase of the number of tube row. Fig. 5(c) shows that the Colburn $j_m$ factor decreases with the increase of inlet relative humidity. The baddish mass transfer characteristic might be resulted from forming of thicker condensate water film on the fin surface when the inlet relative humidity of air increases.

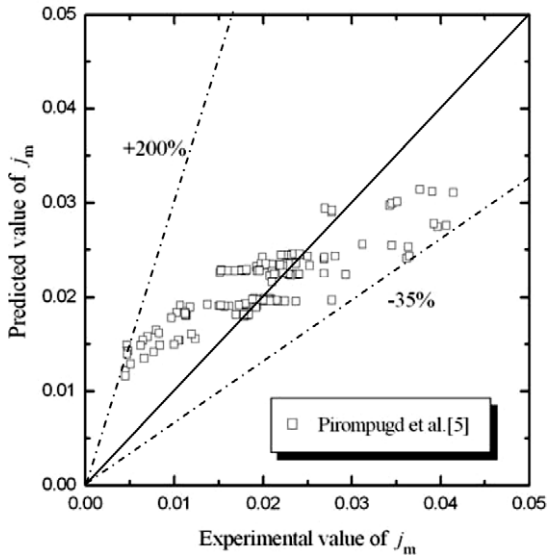


**Fig. 7.** Validation of existing mass transfer model with experiment data.

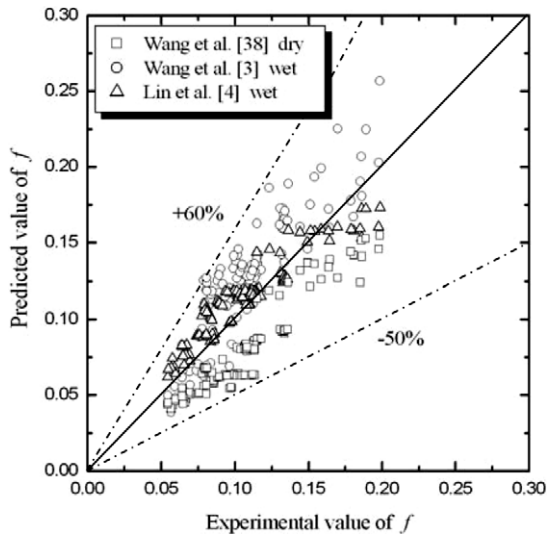


**Fig. 8.** Validation of existing friction correlations with experiment data.

## 5. Correlations

### 5.1. Predictability verification of existing correlations to experimental data

The available airside heat transfer correlations of wavy fin include Webb correlation [34], Kim et al. correlation [35] and Wang et al. correlations [24,36–38] for dry condition, and Wang et al. correlation [3], Lin et al. correlation [4] and Pirompugd et al. correlation [5] for dehumidifying condition. The available airside mass transfer correlation in open literatures is only Pirompugd et al. correlation [5]. All the above mentioned heat and mass transfer correlations were developed on the wavy fin without hydrophilic coating.

Fig. 6(a) depicts comparison of predicted values of dry condition correlations with present experimental data. It shows that both Webb correlation [34] and Kim et al. [35] over-predict the experimental data. Wang et al. [38] indicated that the over-prediction may be attributed to the data-source of Beecher and Fagan [39]. A series of investigation of the wavy patterns based on commercially available samples were conducted by Wang et al. [24,25,36,38]. They presented separated correlations applicable to larger diameter tubes ($D_o$ = 12.7, 15.88 mm, before expansion) and smaller diameter tubes ($D_o$ = 7.94, 9.53 mm, before expansion). Wang et al. correlation [38] is developed using the experimental data by Wang et al. [25,36,37], and it has the most wide application range for wavy fin-and-tube heat exchanger under dry condition at present. Fig. 6(a) also shows the comparison of predicted values of Wang et al. correlations [38] with present experimental data. It shows that Wang et al. correlation [38] over-predict the experimental data.

Fig. 6(b) shows comparison of the experimental data with predicted values of dehumidifying condition correlations. As shown in

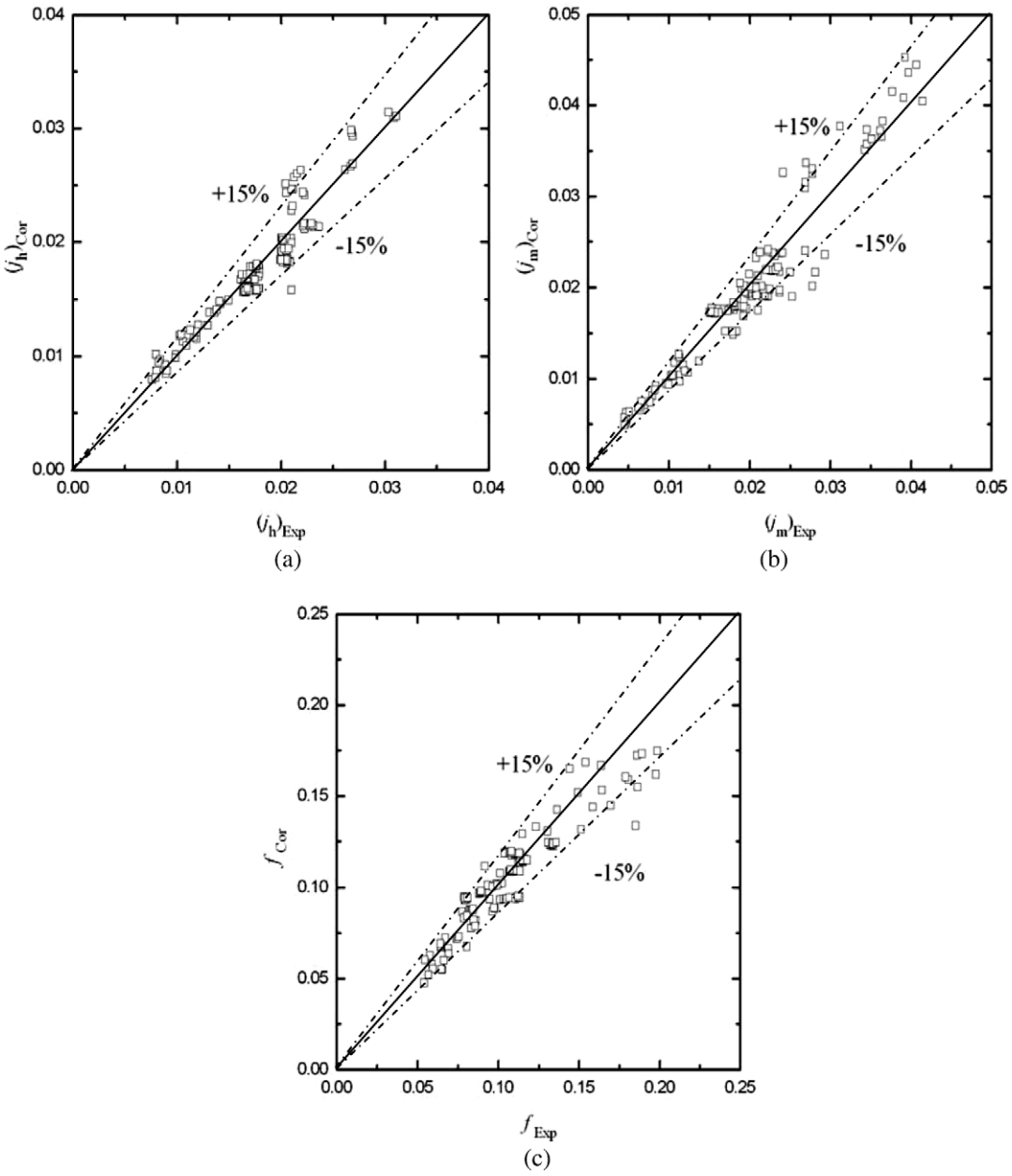


**Fig. 9.** Comparison of the proposed heat/mass and momentum transfer correlations with experimental data of wavy fin with hydrophilic coating under wet conditions (a) $j_h$ (b) $j_m$ (c) $f$.

Fig. 6(b), Wang et al. correlation [3] and Pirompugd et al. correlation [5] slightly over-predict the experimental data. The reason may be related to the condensate condition on the fin surface. For wavy fin without hydrophilic coating, the condensate water can exist on the fin surface with the form of droplets, which can act as the effect of "rough surface" and enhance the airside heat transfer. Fig. 6(b) also shows that Lin et al. correlation [4] cannot predict the experimental data satisfactorily, because the experimental object of Lin et al. [4] is single wavy fin instead of wavy fin-and-tube heat exchanger.

Fig. 7 shows comparison of the Pirompugd et al. mass transfer correlation [5] with the experimental data. It shows that the Pirompugd et al. correlation [5] over-predict the experimental data. Possible reason is as follows. For fin without hydrophilic coating, the condensate water droplets will make more space for mass transfer between air and fin surface; but for fin with hydrophilic coating, the condensate water exist on the fin surface with the form of film, which will reduce the mass transfer space and decrease the mass transfer performance.

The available momentum transfer correlations include Wang et al. correlation [24,25,38,39] for dry condition and Wang et al. correlation [3], Lin et al. correlation [4] for dehumidifying condition. Fig. 8 indicates the comparison of the experimental data with the predict value. It shows that momentum transfer correlations for dry condition low-predict the pressure drop characteristic of wavy fin-and-tube heat exchanger with hydrophilic coating under dehumidifying condition. The reason is as follows. Although the condensate water comes into being the film on the fin surface, it can still block the flow of air and increase the airside pressure drop. The comparisons of the experimental data with the predicted value of wet condition correlation are also shown in Fig. 8, which depict that the momentum transfer correlations used for uncoated fin over-predict the experimental data. The reason is that the airside pressure drop raised by water droplets on the uncoated fin surface is bigger than that by water film on the coated fin surface.

Above evaluation show that the available heat, mass and momentum correlations cannot predict the airside heat transfer, mass transfer and pressure drop characteristic of wavy fin-and-tube heat exchanger with hydrophilic coating under dehumidifying condition satisfactorily. It is necessary to develop new correlation to describe the airside performance better.

### 5.2. New correlations development

Based on the experimental data, a multiple linear regression technique in a practical range of experimental data ($350 < Re_{Dc} < 4500$) was carried out, and the appropriate correlation form of $j_h$, $j_m$ and $f$ are given as follows:

$$j_h = 0.3266 Re_{Dc}^{-0.5435} \left(\frac{P_t}{P_l}\right)^{0.1399} \left(\frac{F_p}{D_c}\right)^{-0.7482} N^{-0.6314} \quad (33)$$

$$j_m = 2.6915 Re_{Dc}^{-0.9098} \left(\frac{P_t}{P_l}\right)^{0.6632} \left(\frac{F_p}{D_c}\right)^{-0.6844} N^{0.0219} \quad (34)$$

$$f = 2.0056 Re_{Dc}^{-0.4935} \left(\frac{P_t}{P_l}\right)^{-0.3782} \left(\frac{F_p}{D_c}\right)^{-0.3958} N^{-0.2039} \quad (35)$$

The applicability ranges for Eqs. (33)–(35) are listed as follows:

$Re_{Dc}$ 350–4500
$P_t$ 21.0–25.4 mm
$P_l$ 19.05 mm
$D_c$ 7.51–10.31 mm
$F_p$ 1.2–1.8 mm
$N$ 2–3

**Table 4**
Comparison of the proposed correlation with experimental data.[a,b]

| Deviation | $j_h$ (%) | $j_m$ (%) | $f$ (%) |
|---|---|---|---|
| ±10% | 78.9 | 60.9 | 68.8 |
| ±15% | 90.6 | 82.1 | 85.9 |
| ±20% | 95.3 | 92.9 | 97.7 |
| ±25% | 99.2 | 96.9 | 99.2 |
| Mean deviation | 6.3 | 8.9 | 7.9 |

[a] Mean deviation = $\frac{1}{M}\left(\sum_1^M \frac{|\text{Correlation}-\text{Data}|}{\text{Data}}\right) \times 100\%$.
[b] $M$, number of data point.

As shown in Fig. 9, the proposed heat transfer $j_h$ factor correlation, mass transfer $j_h$ factor correlation and momentum transfer $f$ factor correlation can correlate 90.6%, 82.1% and 85.9% of the test data within ±15% deviation limit, and have a mean deviation of 6.3%, 8.9% and 7.9%, respectively. Detailed comparisons between the proposed correlations and the experimental data are depicted in Table 4.

## 6. Conclusion

The airside heat, mass and momentum transfer performance of compact wavy fin-and-tube heat exchanger with hydrophilic coating under dehumidifying conditions were presented and discussed in this study. A total of seven fin-and-tube heat exchangers having wavy fin geometry were tested. The following conclusions are obtained:

- The process line on psychrometric chart of fin-and-tube heat exchanger for partially wet conditions and more accurate overall heat transfer coefficient calculation equation are put forward.
- The Colburn $j_h$ factor and the Colburn $j_m$ factor decrease with the increase of the fin pitch. This phenomenon becomes more pronounced at lower Reynolds number, and the friction factor is very sensitive to change in fin pitch. The friction factor shows a cross-over phenomenon as fin pitch changes.
- The Colburn $j_h$ factor decreases with the increase of the number of tube rows, and this phenomenon is more pronounced as Reynolds number decrease. The Colburn $j_m$ factor increases with the increase of the number of tube rows. The friction performance is insensitive to the change of the number of tube rows.
- The effects of inlet relative humidity on the heat transfer and friction performance can be omitted, but the Colburn $j_m$ factor decreases with the increase of the number of tube rows.
- The state-of-the-art heat, mass and momentum transfer correlations to experimental data can not well predict the experimental results.
- The new heat, mass and momentum transfer correlations have been proposed to describe the present test results according to the multiple linear regression technique. The mean deviations of the proposed $j_h$, $j_m$ and $f$ correlations are 6.3%, 8.9% and 7.9%, respectively.

## Acknowledgment

The authors are very grateful to Dr. C.C. Wang of ITRI, Taiwan for giving advices and documents on experimental rig design and correlation development for this study.

## Appendix A. Wet fin efficiency calculation

*For. fully wet conditions*

$$\eta_{f,fullywet} = \frac{2r_i M^*(T_{fb} - T_a^*)}{M_{fb}^2(r_o^2 - r_i^2)(T_a - T_{fb})} \cdot \left[\frac{K_1(M^*r_o)I_1(M^*r_i) - I_1(M^*r_o)K_1(M^*r_i)}{K_1(M^*r_o)I_0(M^*r_i) + K_0(M^*r_i)I_1(M^*r_o)}\right] \quad (A1)$$

where

$$M^{*2} = \frac{2h_s}{k_f\delta_f}(1 + b\beta) \quad (A2)$$

$$M_{fb}^2 = \frac{2h_s}{k_f\delta_f}\left(1 + \beta\frac{W_a - W_{s,f}}{T_a - T_f}\right) \quad (A3)$$

$$T_a^* = \frac{T_a + \beta \cdot W_a - a\beta}{1 + b\beta} \quad (A4)$$

$$\beta = \frac{i_{fg}}{RC_{p,a}} \quad (A5)$$

In the calculation, coefficients $a$, $b$ and the fin tip temperature $T_{ft}$ need to be iterated. $T_{ft}$ can be calculated by Eq. (A6). When $T_{fb}$ and $T_{ft}$ are specified, if the fin is totally wet ($T_{ft} \leqslant T_{a,d}$), the values of $a$ and $b$ can be readily determined with Eqs. (A7) and (A8). If the fin is partially wet ($T_{fb} \leqslant T_{a,d} \leqslant T_{ft}$), the values of $a$ and $b$ can be determined according to $T_{fb}$ and $T_{a,d}$.

$$T_f = T_a^* + (T_{fb} - T_a^*)\left[\frac{K_1(M^*r_o)I_0(M^*r) + I_1(M^*r_o)K_0(M^*r)}{K_0(M^*r_i)I_1(M^*r_o) + K_1(M^*r_o)I_0(M^*r_i)}\right] \quad (A6)$$

$$W_{s,f} = a + bT_f \quad (A7)$$

$$W_{s,f} = (3.7444 + 0.3078T_f + 0.0046T_f^2 + 0.0004T_f^3) \times 10^{-3} \quad 0 \leq T_f \leq 30^{\circ}C \quad (A8)$$

*For. partially wet conditions*

$$\eta_{f,partiallywet} = \frac{2r_i M^*}{M_{fb}^2(r_o^2 - r_i^2)(T_a - T_{fb})} \times \left\{\left[\frac{I_1(M^*r_i)K_0(M^*\xi) + I_0(M^*\xi)K_1(M^*r_i)}{I_0(M^*r_i)K_0(M^*\xi) - I_0(M^*\xi)K_0(M^*r_i)}\right](T_{fb} - T_a^*) - \left[\frac{I_0(M^*r_i)K_1(M^*r_i) + I_1(M^*r_i)K_0(M^*r_i)}{I_0(M^*r_i)K_0(M^*\xi) - I_0(M^*\xi)K_0(M^*r_i)}\right](T_{dew} - T_a^*)\right\} \quad (A9)$$

The parameter $\xi$ in Eq. (A9) is the boundary line between dry region and wet region. It can be determined from the continuity of heat flow at the point separating the dry and wet surfaces.

$$\left.\frac{dT_f}{dr}\right|_{r=\xi^-} = \left.\frac{dT_f}{dr}\right|_{r=\xi^+} \quad (A10)$$

The fin surface temperature distribution at dry region and wet region in Eq. (A10) can be seen as following.

For wet region

$$T_f = T_a^* + \left[\frac{I_0(M^*r)K_0(M^*\xi) - I_0(M^*\xi)K_0(M^*r)}{I_0(M^*r_i)K_0(M^*\xi) - I_0(M^*\xi)K_0(M^*r_i)}\right](T_{fb} - T_a^*) + \left[\frac{I_0(M^*r_i)K_0(M^*r) - I_0(M^*r)K_0(M^*r_i)}{I_0(M^*r_i)K_0(M^*\xi) - I_0(M^*\xi)K_0(M^*r_i)}\right](T_{dew} - T_a^*) \quad (A11)$$

$$\left.\frac{dT_f}{dr}\right|_{r=\xi^-} = M^*\left[\frac{I_1(M^*\xi)K_0(M^*\xi) + I_0(M^*\xi)K_1(M^*\xi)}{I_0(M^*r_i)K_0(M^*\xi) - I_0(M^*\xi)K_0(M^*r_i)}\right](T_{fb} - T_a^*) - M^*\left[\frac{I_0(M^*r_i)K_1(M^*\xi) + I_1(M^*\xi)K_0(M^*r_i)}{I_0(M^*r_i)K_0(M^*\xi) - I_0(M^*\xi)K_0(M^*r_i)}\right](T_{dew} - T_a^*) \quad (A12)$$

For dry region

$$T_f = T_a + (T_{dew} - T_a) \times \left[\frac{K_1(m^*r_o)I_0(m^*r) + I_1(m^*r_o)K_0(m^*r)}{K_0(m^*\xi)I_1(m^*r_o) + K_1(m^*r_o)I_0(m^*\xi)}\right] \quad (A13)$$

$$\left.\frac{dT_f}{dr}\right|_{r=\xi^+} = (T_{dew} - T_a)m^*\left[\frac{K_1(m^*r_o)I_1(m^*\xi) - I_1(m^*r_o)K_1(m^*\xi)}{K_0(m^*\xi)I_1(m^*r_o) + K_1(m^*r_o)I_0(m^*\xi)}\right] \quad (A14)$$

where

$$m^{*2} = \frac{2h_s}{k_f \cdot \delta_f} \quad (A15)$$

## References


[1] D.R. Mirth, S. Ramadhyani, Prediction of cooling-coils performance under condensing conditions, Int. J. Heat Fluid Flow 14 (4) (1993) 391–400.
[2] D.R. Mirth, S. Ramadhyani, Correlations for predicting the air-side Nusselt numbers and friction factors in chilled-water cooling coils, Exp. Heat Transfer 7 (2) (1994) 143–162.
[3] C.C. Wang, Y.J. Du, Y.J. Chang, W.H. Tao, Airside performance of herringbone fin-and-tube heat exchangers in wet conditions, Can. J. Chem. Eng. 77 (6) (1999) 1225–1230.
[4] Y.T. Lin, Y.T. Hwang, C.C. Wang, Performance of the herringbone wavy fin under dehumidifying conditions, Int. J. Heat Mass Transfer 45 (25) (2002) 5035–5044.
[5] W. Pirompugd, S. Wongwises, C.C. Wang, Simultaneous heat and mass transfer characteristics for wavy fin-and-tube heat exchangers under dehumidifying conditions, Int. J. Heat Mass Transfer 49 (1–2) (2006) 132–143.
[6] M. Mimaki, Effectiveness of finned tube heat exchanger coated hydrophilic-type film, ASHRAE Trans. 93 (1987) 62–71.
[7] K. Hong, Fundamental characteristics of dehumidifying heat exchangers with and without wetting coating, Ph.D. Thesis, Department of mechanical engineering, the Pennsylvania State University, U.S.A., 1996.
[8] K. Hong, R.L. Webb, Wetting coatings for dehumidifying heat exchangers, Int. J. HVAC Res. 6 (3) (2000) 229–239.
[9] K. Hong, R.L. Webb, Performance of dehumidifying heat exchangers with and without wetting coating, ASME J. Heat Transfer 121 (4) (1999) 1018–1026.
[10] C.C. Wang, C.T. Chang, Heat and mass transfer for plate fin-and-tube heat exchangers, with and without hydrophilic coating, Int. J. Heat Mass Transfer 41 (1998) 3109–3120.
[11] C.C. Wang, W.S. Lee, W.J. Sheu, Y.J. Chang, A comparison of the airside performance of the fin-and-tube heat exchangers in wet conditions; with and without hydrophilic coating, Appl. Thermal Eng. 22 (2002) 269–278.
[12] ASHRAE Standard 41.2-1987, Standard Methods for Laboratory Air-flow Measurement, Atlanta: American Society of Heating, Refrigerating and Air-Conditioning Engineers, Inc., 1987.
[13] R.J. Moffat, Describing the uncertainties in experimental results, Exp. Thermal Fluid Sci. 1 (1) (1988) 3–17.
[14] L. Threlkeld, Thermal Environment Engineering, Prentice-Hall, New York, 1970. pp. 257–259.
[15] ASHRAE Standard, Method of Testing Forced Circulation Air Cooling and Air Heating Coils, American Society of Heating, Refrigerating and Air-Conditioning Engineers, Inc., Atlanta, GA, 2000.
[16] T.R. Bump, Average temperature in simple heat exchangers, ASME J. Heat Transfer 85 (2) (1963) 182–183.
[17] R.J. Myers, The effect of dehumidification on the air-side heat transfer coefficient for a finned-tube coil, M.S. Thesis, University of Minnesota, Minneapolis, 1967.
[18] C.C. Wang, Y.C. Hsieh, Y.T. Lin, Performance of plate finned tube heat exchangers under dehumidifying conditions, ASME J. Heat Transfer (119) (1997) 109–117.
[19] V. Gnielinski, New equation for heat and mass transfer in turbulent pipe and channel flow, Int. Chem. Eng. 16 (1976) 359–368.
[20] X. Ma, G. Ding, Y. Zhang, K. Wang, Airside heat transfer and friction characteristics for enhanced fin-and-tube heat exchanger with hydrophilic coating under wet conditions, Int. J. Refrig. 30 (7) (2007) 1153–1167.
[21] W.M. Kays, A.L. London, Compact Heat Exchanger, third ed., McGraw-Hill, New York, 1984.
[22] D.G. Rich, The effect of fin spacing on the heat transfer and friction performance of multi-row, plate fin-and-tube heat exchangers, ASHRAE Trans. 79 (2) (1973) 137–145.
[23] C.C. Wang, Y.J. Chang, Y.C. Hsieh, Y.T. Lin, Sensible heat and friction characteristics of plate fin-and-tube heat exchangers having plane fins, Int. J. Refriger. 19 (4) (1996) 223–230.
[24] C.C. Wang, W.L. Fu, C.T. Chang, Heat transfer and friction characteristics of typical wavy fin-and-tube heat exchangers, Exp. Thermal Fluid Sci. 14 (2) (1997) 174–186.

[25] C.C. Wang, Y.M. Tsi, D.C. Lu, Comprehensive study of convex-louver and wavy fin-and-tube heat exchangers, J. Thermophys. Heat Transfer 12 (3) (1998) 423–430.
[26] C.C. Wang, Y.P. Chang, K.U. Chi, Y.J. Chang, An experimental study of heat transfer and friction characteristics of typical louver fin-and-tube heat exchangers, Int. J. Heat Mass Transfer 41 (4–5) (1998) 817–822.
[27] C.C. Wang, K.Y. Chi, Heat transfer and friction characteristics of plain fin-and-tube heat exchangers, Part I: new experimental data, Int. J. Heat Mass Transfer 43 (15) (2000) 2681–2691.
[28] K. Torikoshi, G. Xi, Y. Nakazawa, H. Asano, Flow and heat transfer performance of a plate-fin and tube heat exchanger (1st report: effect of fin pitch), in: 10th Int. Heat Transfer Conf. 1994, paper 9-HE-16, 1994, pp. 411–416.
[29] D.G. Rich, The effect of the number of tube rows on the heat transfer performance of smooth plate fin-and-tube heat exchangers, ASHRAE Trans. 81 (1) (1975) 307–317.
[30] C.C. Wang, W.S. Lee, W.J. Sheu, Y.J. Chang, Parametric study of the air-side performance of slit fin-and-tube heat exchangers in wet conditions, in: Proceedings of the Institution of Mechanical Engineers, Part C: Journal of Mechanical Engineering Science, vol. 215(9), 2001, pp. 1111–1122.
[31] C.C. Wang, Y.T. Lin, C.J. Lee, Heat and momentum transfer for compact louvered fin-and-tube heat exchangers in wet conditions, Int. J. Heat Mass Transfer 43 (18) (2000) 3443–3452.
[32] W.L. Fu, C.C. Wang, C.T. Chang, Effect of anti-corrosion coating on the thermal characteristics of a louvered finned heat exchanger under dehumidifying condition, Adv. Enhanced Heat/Mass Transfer Energy Efficiency (1995) 75–81.
[33] T. Yoshii, M. Yamamoto, T. Otaki, Effects of dropwise condensate on wet surface heat transfer of air cooling coils, in: Proceedings of the 13th International Congress of Refrigeration, International Institute of Refrigeration, Paris, France, 1973, pp. 285–292.
[34] R.L. Webb, Air-side heat transfer correlations for flat and wavy plate fin-and-tube geometries, ASHRAE Trans. 96 (2) (1990) 445–449.
[35] N.H. Kim, J.H. Yun, R.L. Webb, Heat transfer and friction correlations for wavy plate fin-and-tube heat exchangers, J. Heat Transfer 119 (3) (1997) 560–567.
[36] C.C. Wang, J.Y. Jang, N.F. Chiou, A heat transfer and friction correlation for wavy fin-and-tube heat exchangers, Int. J. Heat Mass Transfer 42 (10) (1999) 1919–1924.
[37] C.C. Wang, Y.T. Lin, C.J. Lee, Y.J. Chang, Investigation of wavy fin-and-tube heat exchangers: a contribution to databank, Exp. Heat Transfer 12 (1) (1999) 73–89.
[38] C.C. Wang, Y.M. Hwang, Y.T. Lin, Empirical correlations for heat transfer and flow frictions characteristics of herringbone wavy fin-and-tube heat exchangers, Int. J. Refriger. 25 (5) (2002) 673–680.
[39] D.T. Beecher, T.J. Fagan, Effects of fin pattern on the air-side heat transfer coefficient in plate finned-tube heat exchangers, ASHRAE Trans. 93 (2) (1987) 1961–1984.